Research Paper

Electrophilic characteristics and aqueous behavior of fatty acid nitroalkenes

Valentina Grippo [a], Milos Mojovic [b], Aleksandra Pavicevic [b], Martin Kabelac [c], Frantisek Hubatka [d], Jaroslav Turanek [d], Martina Zatloukalova [a], Bruce A. Freeman [e], Jan Vacek [a,f,*]

[a] Department of Medical Chemistry and Biochemistry, Faculty of Medicine and Dentistry, Palacky University, Hnevotinska 3, Olomouc, 775 15, Czech Republic
[b] Faculty of Physical Chemistry, University of Belgrade, Studentski Trg 12-16, Belgrade, Serbia
[c] Department of Chemistry, Faculty of Science, University of South Bohemia, Branisovska 31, Ceske Budejovice, 370 05, Czech Republic
[d] Department of Pharmacology and Immunotherapy, Veterinary Research Institute, v.v.i., Hudcova 70, 621 00, Brno, Czech Republic
[e] Department of Pharmacology and Chemical Biology, University of Pittsburgh School of Medicine, Pittsburgh, PA, 15261, USA
[f] The Czech Academy of Sciences, Institute of Biophysics, Kralovopolska 135, Brno, 612 65, Czech Republic

ARTICLE INFO

ABSTRACT

Fatty acid nitroalkenes (NO$_2$-FA) are endogenously-generated products of the reaction of metabolic and inflammatory-derived nitrogen dioxide (·NO$_2$) with unsaturated fatty acids. These species mediate signaling actions and induce adaptive responses in preclinical models of inflammatory and metabolic diseases. The nitroalkene substituent possesses an electrophilic nature, resulting in rapid and reversible reactions with biological nucleophiles such as cysteine, thus supporting post-translational modifications (PTM) of proteins having susceptible nucleophilic centers. These reactions contribute to enzyme regulation, modulation of inflammation and cell proliferation and the regulation of gene expression responses. Herein, focus is placed on the reduction-oxidation (redox) characteristics and stability of specific NO$_2$-FA regioisomers having biological and clinical relevance; nitro-oleic acid (NO$_2$-OA), bis-allylic nitro-linoleic acid (NO$_2$-LA) and the conjugated diene-containing nitro-conjugated linoleic acid (NO$_2$-cLA). Cyclic and alternating-current voltammetry and chronopotentiometry were used to the study of reduction potentials of these NO$_2$-FA. R–NO$_2$ reduction was observed around −0.8 V (*vs.* Ag/AgCl/3 M KCl) and is related to relative NO$_2$-FA electrophilicity. This reduction process could be utilized for the evaluation of NO$_2$-FA stability in aqueous milieu, shown herein to be pH dependent. In addition, electron paramagnetic resonance (EPR) spectroscopy was used to define the stability of the nitroalkene moiety under aqueous conditions, specifically under conditions where nitric oxide (·NO) release could be detected. The experimental data were supported by density functional theory calculations using 6–311++G (d,p) basis set and B3LYP functional. Based on experimental and computational approaches, the relative electrophilicities of these NO$_2$-FA are NO$_2$-cLA >> NO$_2$-LA > NO$_2$-OA. Micellarization and vesiculation largely define these biophysical characteristics in aqueous, nucleophile-free conditions. At concentrations below the critical micellar concentration (CMC), monomeric NO$_2$-FA predominate, while at greater concentrations a micellar phase consisting of self-assembled lipid structures predominates. The CMC, determined by dynamic light scattering in 0.1 M phosphate buffer (pH 7.4) at 25 °C, was 6.9 (NO$_2$-LA) 10.6 (NO$_2$-OA) and 42.3 μM (NO$_2$-cLA), respectively. In aggregate, this study provides new insight into the biophysical properties of NO$_2$-FA that are important for better understanding the cell signaling and pharmacological potential of this class of mediators.

1. Introduction

Elevated levels of nitrated amino acids, nucleotides and lipids have been detected in tissues and fluids of patients undergoing inflammatory conditions [1,2]. These derivatives are generated *in vivo* and *in vitro* upon exposure to nitric oxide (·NO)- and nitrite (NO$_2^-$)-derived RS that yield nitrogen dioxide (NO$_2$). For example, ·NO and NO$_2^-$ are precursors for the generation of peroxynitrous acid (ONOOH), nitro-soperoxocarbonate (ONOOCO$_2$) and dinitrogen trioxide (N$_2$O$_3$). Also, NO$_2^-$ can be oxidized by heme peroxidases to yield ·NO$_2$ [3–5]. When ·NO$_2$ reacts with the double bond of an unsaturated acyl chain, forming

Abbreviations

ACV	alternating-current voltammetry
cLA	conjugated-linoleic acid
CMC	critical micellar concentration
CPSA	chronopotentiometric stripping analysis
CV	cyclic voltammetry
DFT	density functional theory
DLS	dynamic light scattering
DTCS	*N*-(dithiocarboxy)sarcosine
HMDE	hanging mercury drop electrode
EPR	electron paramagnetic resonance

FA	fatty acids
LA	linoleic acid
MM	molecular modelling
NO_2-cLA	nitro-conjugated-linoleic acid
NO_2-LA	nitro-linoleic acid
NO_2-OA	nitro-oleic acid
OA	oleic acid
PGE	pyrolytic graphite electrode
PMT	post-translational modification
QM	quantum mechanics
RS	reactive species
TCEP	tris(2-carboxyethyl)phosphine hydrochloride.

a nitroalkene substituent, the products have generically been termed nitro-fatty acids (NO_2-FA). NO_2-FA found in living organisms are a result of the nitration of oleic (C18:1) [6], linoleic (C18:2) [7], linolenic (C18:3) and arachidonic (C20:4) [8] acids. Current data supports that NO_2-FA display anti-inflammatory and adaptive signaling actions. The administration of synthetic natural and non-natural nitroalkenes also can mitigate pathogenic responses in preclinical models of cardiovascular, ischemic, metabolic, inflammatory and fibrotic diseases [9–12].

NO_2-FA undergo reversible Michael addition [13] with cellular nucleophiles, predominantly Cys, that frequently reside in functionally-significant cell signaling, metabolic and transcriptional regulatory proteins. The nitro group on the alkene moiety has a strong electron-withdrawing behavior that confers electron deficiency to the β-carbon and responsiveness to nucleophilic attack by thiolates. In nitro-conjugated linoleic acid, both the β- and δ-carbons with respect to the nitro group are susceptible to Michael addition [14]. The β-adduct is the kinetic product while the δ-adduct is the thermodynamic product. This Michael addition is reversible and kinetically rapid, which differentiates the NO_2-FA from other endogenous signaling electrophiles (such as aldehydic fatty acid oxidation products and cyclopentenone prostaglandins) that react slowly and irreversibly with nucleophiles [15, 16].

NO_2-FA show NO donor activities *in vitro* [17–19]. The mechanism(s) underlying aqueous NO release by nitroalkenes has not been definitively established, but may include a modified Nef reaction. A possible mechanism is that under neutral aqueous conditions, the nitroalkene facilitates the formation of the nitronate anion; then followed by protonation and deprotonation steps resulting in a nitroso intermediate. This nitroso intermediate has a weak C–N bond that yields ·NO [20]. The presence of the nitrite radical was supported by chemiluminescence measurements and EPR-based methodologies [21]. It is noted that in these aqueous-based NO donor studies and buffer-perfused vascular rings that claim a vasodilatory action of NO_2-FA, experimental results might have been complicated by a) contaminating nitrite in NO_2-FA preparations or b) unique reactions that occur in pure aqueous milieu as opposed to those operative in more complex biological fluids and tissues. For example, extensive preclinical pharmacokinetics and toxicology studies, as well as human Phase 1 and Phase 2 trials do not show an acute effect of intravenous or oral NO_2-FA on blood pressure or pulse rate, suggesting that NO and cGMP-dependent signaling mechanisms have not been engaged (unpublished). In any event, these previous studies motivated the present more detailed analysis of the kinetics of NO generation by fatty acid nitroalkenes and mitigating factors.

The endogenous formation of NO_2-FA [3–5] will be strongly influenced by diet, which may contain pre-formed NO_2-FA or a combination of precursor fatty acids and sources of the organic nitrates required for fatty acid nitration (i.e., NO_2^- coming from animal and plant-derived products or NO_2^--based preservatives) [22]. Clinical studies have revealed that dietary supplementation of organic nitrates, with and without co-administration of conjugated linoleic acid (cLA), resulted in

a sustained level of NO_2-cLA only when cLA was co-administered [23]. This indicates that cLA is rate limiting and its simultaneous presence in the gastric compartment together with NO_2^- and its precursor nitrate (NO_3^-) is needed for the formation of the NO_2-cLA. Related to this, the cardiovascular health-promoting properties attributed to the Mediterranean diet may be due in part to these dietary constituents that could react and upregulate NO_2-FA generation [24–26]. Thus, interest in characterizing the biophysical and biochemical properties of NO_2-FA has grown [27].

The detailed formation, metabolism, distribution and excretion of NO_2-FA, as well as the mechanisms accounting for net signaling responses to NO_2-FA are still not fully resolved [7,20,28]. From a methodological point of view, NO_2-FA are complex analytes because of aqueous insolubility, an amphiphilic nature, a net negative charge and different chemical reactivities in aqueous and lipophilic biological microenvironments. MS-based approaches [29] as well as spectrophotometry and crystallographic analysis [21] have been used for structural characterization and quantification of unesterified NO_2-FA, with mass spectrometry using electrospray ionization (ESI) coupled with liquid chromatography (LC-MS) being the most suitable method [20,30].

Herein, we expand on a previous study [31] and compare the biophysical properties of NO_2-OA, NO_2-LA and NO_2-cLA (Scheme 1) using multiple analytical and computational approaches. Native FA without NO_2 substitution (OA, LA and cLA) served as negative controls in all experiments. These analyses define the reactivity, stability, NO release characteristics, conformational properties and micellarization of key NO_2-FA.

2. Experimental

2.1. Chemicals

Chemicals were purchased from Merck KGaA (Darmstadt, Germany) or BioRad Laboratories (Hercules, CA, USA). 10-nitrolinoleate (NO_2-LA) as pure positional isomer was from Cayman Chemical (Ann Arbor, MI, USA). NO_2-OA as an equimolar mixture of the 9- and 10-nitrooctadec-(9)-enoic acid and NO_2-cLA as an equimolar mixture of the 9- and 12-nitrooctadeca-(9,11)-dienoic acid were synthesized as previously [32]. The purity of NO_2-FA was higher than 98% for all samples. The stock solutions were prepared using methanol. With exception of NO_2-LA, NO_2-OA and NO_2-cLA were used throughout the study as an appropriate mixture of both positional isomers (Scheme 1). The unmodified fatty acids (LA, cLA and OA) were purchased from Merck KGaA (Darmstadt, Germany). All solutions were prepared using Milli-Q water (18.2 MΩ cm^{-1}), Millipore, Bedford, MA, USA. All other used chemicals were of analytical grade.

2.2. CMC determination by DLS

The micelles were prepared by dissolving individual fatty acids and
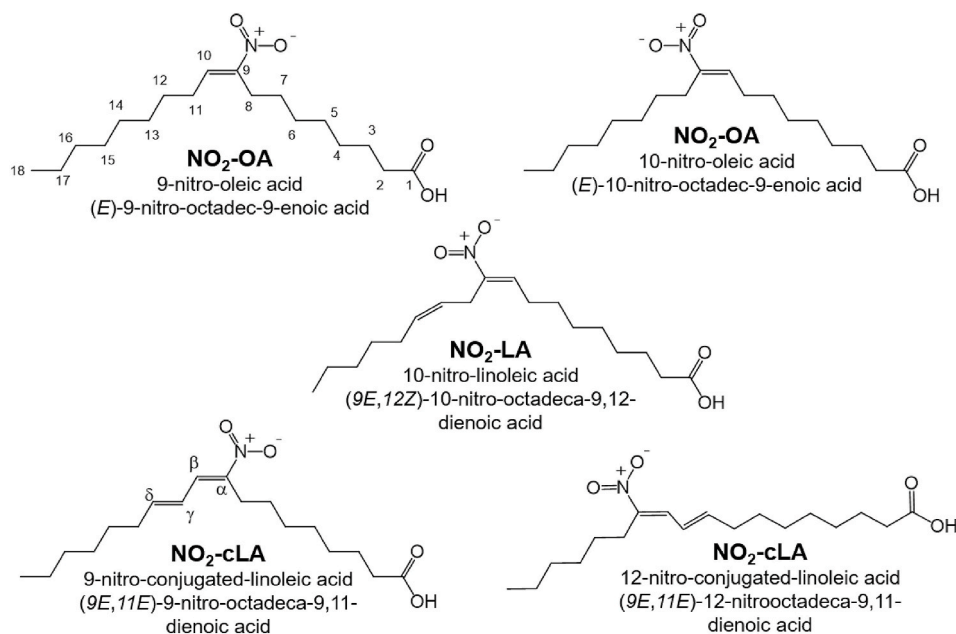
Scheme 1. Structures and identification of NO$_2$-FA used in this study.

their nitro derivatives in 1 mM NaOH solution [33]. Each solution was diluted to the final concentration of 100 μM fatty acid (as sodium salt) with 0.1 M phosphate buffer (pH 7.4). Samples were diluted to several lower concentrations before performing the experiments. Dynamic light scattering (DLS) measurements were performed using Zetasizer Nano ZSP (Malvern Panalytical Ltd, Malvern, UK) at 25 °C. Finally, light scattering intensities (Derived Count Rate, Kcps) were plotted against solute concentration. Critical micellar concentration (CMC) was determined as the intersection between the straight line coming from the light scattering intensity values below CMC with the straight line derived from the light scattering intensities above CMC (region of rapid intensity increase) [34].

2.3. Electrochemistry

All electrochemical measurements were performed at room temperature with a μAutolab III analyzer (EcoChemie, Utrecht, Netherlands) in a three-electrodes cell with an Ag/AgCl/3 M KCl electrode as the reference and platinum wire as the auxiliary electrode. Two types of working electrodes were used: HMDE (hanging mercury drop electrode; area 0.4 mm^2) for constant-current chronopotentiometric stripping analysis (CPSA) and alternating-current voltammetry (ACV), and PGE, a basal-plane pyrolytic graphite electrode (electrode area 9 mm^2, Momentive Performance Materials, USA) for cyclic voltammetry (CV). Individual settings for electrochemical experiments, as well as concentrations of the compounds, are given in the Fig. legends. The electrochemical analyses were performed using two supporting electrolytes: 0.1 M phosphate and Britton-Robinson buffers [35]. For the voltammetry of NO$_2$-FA, all electrolytes were purged with argon. Degassing was not employed with CPSA because the dioxygen does not interfere with the technique. The pH measurements were performed with a HI 2211 pH/ORP Meter (HANNA instruments, IT).

2.4. Stability of NO$_2$-FA

The stability of 8 μM NO$_2$-FA solutions was investigated following the decrease in intensity of the NO reduction peak for more than 24 h by using CPSA. The compounds investigated were dissolved in Britton-Robinson buffer as supporting electrolyte at pH 5, 7.4 and 9 in the presence of atmospheric oxygen. Incubation and CPSA were performed

at 25 °C (controlled by thermostat) and room temperature, respectively.

2.5. Detection of ·NO release from NO$_2$-FA

In order to study whether NO$_2$-FA are able to release ·NO, the Fe(II)(DTCS)$_2$ complex consisting of Fe^{2+} and *N*-(dithiocarboxy)sarcosine, DTCS (Chemos Cz, Prague, Czech Republic) was used as an ·NO- trapping agent. For all three of NO$_2$-FA, 150 mM ethanol stock solutions were prepared. DTCS was dissolved in water and bubbled with N$_2$ for at least 30 min to remove O$_2$. For the purpose of EPR measurements, water solutions of FeSO$_4$ × 7H$_2$O (final concentration 4 mM) and DTCS (final concentration 5.5 mM) were added to Britton-Robinson buffer (pH 7.4), followed by adding small volume of NO$_2$-cLA, NO$_2$-LA or NO$_2$-OA ethanol stock solutions (final concentration 25 mM). Final samples were drawn into gas-permeable Teflon tubes (Zeus Industrial Products, Orangeburg, SC, USA), and placed into the SHQE EPR resonator cavity. Between the measurements, all of the samples were kept at 25 °C. Since ·NO production from NO$_2$-OA has already been inspected [31], previous work was used as a reference.

2.6. EPR data acquisition and processing

EPR spectra were recorded using a Bruker Elexsys II E540 EPR X-band spectrometer (Germany) at 9.85 GHz and 10 mW microwave power. For all measurements, the modulation amplitude was 2 G, modulation frequency 100 kHz, conversion time 14.65 ms and sweep width was 77 G.

2.7. Theoretical calculations

Since the finding of global energy minimum for OA by systematical torsion search was found to be too time consuming and impractical in our previous work [31], a limited set of twenty energetically favorable structures was generated by program FROG2 [36]. This program allows the generation of conformation ensembles of small molecules using a two stage Monte Carlo approach in the dihedral space from initial structure. The conformational search was limited to desired (*E*-, *Z*-) isomers of anionic form of studied FA. The retrieved conformers were further reoptimized at DFT level of theory employing 6–311++G (d, p) basis set and B3LYP functional. Analysis of frontier molecular orbitals

and molecular electrostatic potentials were performed using the program Avogadro [37]. The role of solvent (water, methanol and *n*-octanol) was described in implicit way using PCM model [38]. All quantum mechanical calculations were treated in Gaussian 16 program [39].

3. Results and discussion

3.1. CMC determination by DLS

Fatty acids are amphiphilic molecules with an aliphatic tail which can be either saturated or unsaturated and have a polar headgroup that can be protonated (COOH) or deprotonated (COO⁻). When FA are present in aqueous solution in sufficient amounts near or above their respective critical micellar concentrations (CMC), they can assemble to form micelles, bilayer membranes and liquid-crystalline phases [40]. The formation of these structures is influenced by pH, CO_2 concentration and temperature. The CMC for oleic acid/oleate and linoleic acid/-linoleate in aqueous solution are 6 and 13 μM, respectively [41]. Depending on pH, the nature of self-assembled lipid structures is affected. Sodium oleate forms vesicles at low pH and, with increasing pH the formation of micelles predominates [42] (Table 1). The CMC for sodium cLA varies from 420 μM to 200 μM when pH decreases from 13 to 8.6 [43]. These characteristics are accounted for the interpretation of the chemical reactivities and biochemical properties of NO_2-FA.

First, we measured the CMC of native FA and compared it with the corresponding NO_2-FA derivative (Table 1). The nitro substitution increases the CMC for all NO_2-FA investigated herein. Low CMCs were found for OA and LA and their nitro derivatives; while cLA and NO_2-cLA, had significantly greater CMCs, *i.e.* 22.5 and 42.3 μM, respectively. While the CMC of members of the NO_2-FA class have not yet been reported, it was reported that when NO_2-FA are partitioned in micelles or liposomes. This disposition stabilizes and apparently sequesters the nitro-alkene functional group, as this and limits acid-base catalyzed reactions and concomitant ·NO release and Michael addition of thiols [20,30,44].

3.2. Redox behavior of NO₂-FA

In next experimental work we focused on the redox behavior of NO_2-cLA and NO_2-LA; the redox transformations of NO_2-OA were described recently [31], thus the redox behavior of NO_2-cLA and NO_2-LA was evaluated and compared with NO_2-OA. The redox behavior of NO_2-cLA, an equimolar mixture of the 9- and 12-NO_2 regioisomers was evaluated by cyclic voltammetry (CV) with a basal-plane pyrolytic graphite electrode (PGE) (Fig. 1). Native conjugated-linoleic acid (cLA) was used as a control. The reduction peak (peak NO) of the modified fatty acid is

Table 1

Schematic representation of the self-assembly of fatty acids with respect to critical micellar concentration (CMC). CMC values for free FA and NO_2-FA were determined using density light scattering.

FAs	CMC (μM)
OA	2
NO₂-OA	10.6
LA	5.1
NO₂-LA	6.9
cLA	22.5
NO₂-cLA	42.3
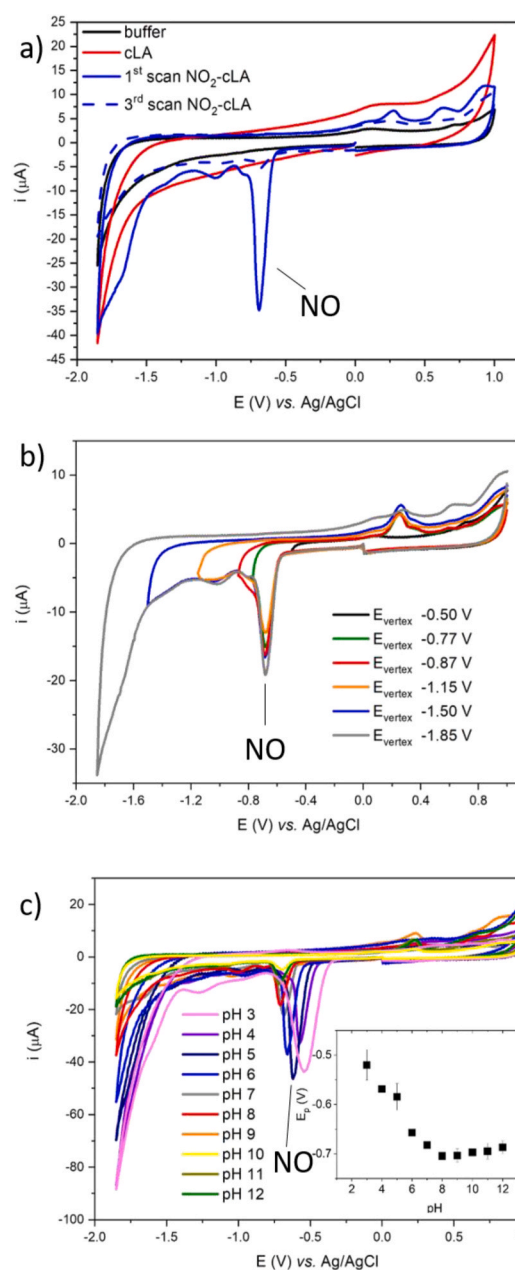
Fig. 1. Cyclic voltammetry (CV) of NO_2-cLA at pyrolytic graphite electrode. (a) CV of 20 μM NO_2-cLA and cLA in 0.1 M phosphate buffer at pH 7.4. CV parameters: initial potential 0 V, first vertex potential −1.85 V, second vertex potential +1 V. (b) CV of 20 μM NO_2-cLA in 0.1 M phosphate buffer at pH 7.4. CV parameters: initial potential 0 V, first vertex potentials −1.85, −1.50, −1.15, −0.87, −0.77, −0.5 V, second vertex potential +1 V. (c) The pH effect on the reduction NO peak coming from 5 μM NO_2-cLA was recorded in Britton-Robinson buffer at pH 3–12. CV parameters: initial potential 0 V, first vertex potential −1.85 V, second vertex potential +1 V. Inset: dependence of the peak NO potential on pH. Prior to the experiments, the electrolytes were deaerated for 10 min with a stream of argon. Time of accumulation $t_A = 30$ s ($E_A = 0$ V), step potential 5 mV and scan rate 1 V/s were applied in all cases. (For interpretation of the references to colour in this figure legend, the reader is referred to the Web version of this article.)

visible at *ca.* −0.8 V in 0.1 M phosphate buffer at pH 7.4 while for the native fatty acid no peak appears (Fig. 1a).

This reduction process is irreversible and of an adsorptive nature [31]. The final reduction product for the nitro moiety has not yet been established but it has been proposed to proceed *via* a hydroxylamine to an amine derivative *via* a complex reduction cascade [20]. For example,

the reduction of *cis*-nitrostilbene in acetonitrile occurs by initial formation of the radical anion followed by irreversible dimerization [45]. When the *trans* isomer was studied, a different mechanism was operative, where the initial radical anion rapidly isomerizes to the *cis* form followed by a partial oxidation to *cis*-nitrostilbene. This process was then followed by the second-order dimerization [45]. The oxidation of individual reduction products of NO_2-cLA can be demonstrated by switching the first vertex potential in CV experiments (Fig. 1b). After reduction of the NO_2 moiety, the anodic peak appears at *ca.* +0.3 V, most probably corresponding to the oxidation of the first reduction product in the cascade. If the potential of −0.5 V (or a less negative one) is applied, the anodic peak was not observed in reverse branch of cyclic voltammograms, (black line, Fig. 1b). The NO reduction peak for the NO_2-cLA acid is also pH dependent, as reported for NO_2-OA (Fig. 1c). The peak NO potential is shifted toward negative values with increasing of pH. In the neutral pH range the maximum of peak current intensity for the reduction process was obtained.

The electrochemical behavior of NO_2-cLA was also studied by constant-current chronopotentiometric stripping analysis (CPSA) with a hanging mercury drop electrode (HMDE). These measurements showed the presence of a second peak (Ads) at negative potential *ca.* −1.3 V (Fig. 2a). Alternating current voltammetry (ACV) at HMDE was used for a more detailed view of the interfacial behavior of NO_2-cLA [46]. Comparison of the out-of-phase (sensitive to adsorption properties) and in-phase (sensible to both diffusion control and adsorption processes) AC voltammograms suggests that peak Ads is most probably due to adsorption/desorption or reorientation processes [31,47]. The out-of-phase ACV shows only a tensametric Ads peak (or double peak) for NO_2-cLA (or cLA). In contrast to in-phase, out-of-phase ACV measurement is not as sensitive to peak NO in agreement with previous findings [31] (Fig. 2b and c). In the same way, the reduction of NO_2-LA was tested and quite similar redox behavior as for NO_2-cLA was found (Fig. 3).

NO_2-cLA redox properties were compared with the corresponding methylene-interrupted diene species (*i.e.* NO_2-LA) and to the monoenoic nitroalkene NO_2-OA by using CPSA. The NO_2-cLA reduction peak NO appears at a less negative potential compared with NO_2-LA and NO_2-OA (Fig. 4a, inset). The same behavior was observed for PGE using the CV method (Fig. 4b). CPS and CV measurements indicated that both conjugated and methylene-interrupted diene containing nitro-linoleic acids have stronger electrophilic character compared with NO_2-OA. This is consistent with the concept that the electrophilic (electron acceptor) properties of NO_2-FA increase with the shift of the NO peak towards less negative potentials.

3.3. Evaluation of NO_2-FA stability

When NO_2-FA electroreduction was inspected over the time, it was apparent that depending on pH, that under aqueous buffer conditions NO_2-FA can undergo decomposition reactions, with a range of pH values (5, 7.4 and 9) showing that the greatest degradation rate was in acidic conditions (Fig. 5). The degradation rate was greater for NO_2-cLA than for NO_2-OA and NO_2-LA, a response consistent with the greater electron acceptor capacity of NO_2-cLA (Fig. 4).

EPR spectroscopy, using Fe(II) $(DTCS)_2$ as the spin-trapping agent, revealed rates and extents of NO_2-cLA and NO_2-LA aqueous decay and generation of ·NO, and allowed comparison with NO_2-OA (Fig. 6). By comparing the EPR signal intensities of spin-adducts, NO_2-cLA generated a significantly greater yield of ·NO than NO_2-LA and NO_2-OA. The amount of ·NO produced by NO_2-LA and NO_2-OA was almost equivalent. The rate constant of ·NO release over 24 h could be calculated for all three NO_2-FA by applying a consecutive reaction fitting model to the kinetic data (Fig. 7, Table 2). This is a simplified model, since multiple simultaneous processes are contributing to the overall kinetics. Namely, this simplified model takes into account the ·NO release from the NO_2-FA, the rapid reaction of ·NO with Fe(II) $(DTCS)_2$, and the decay of the
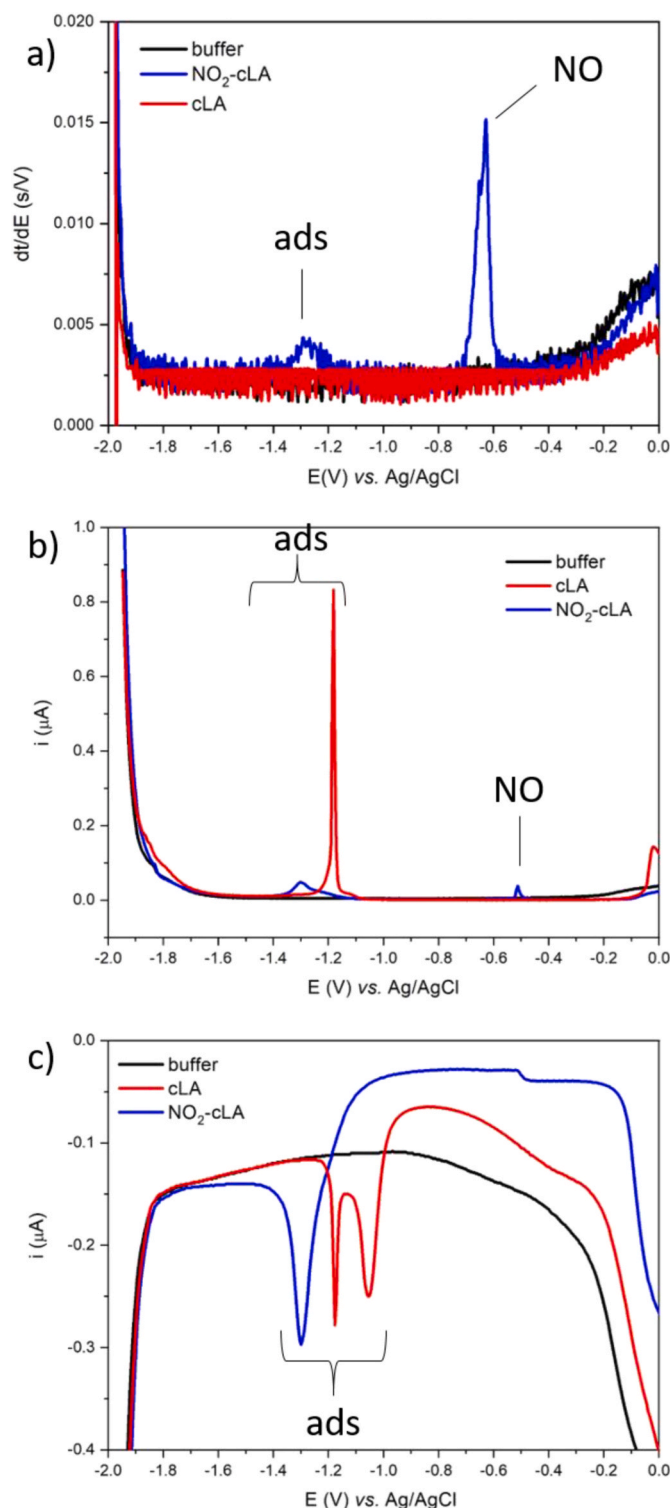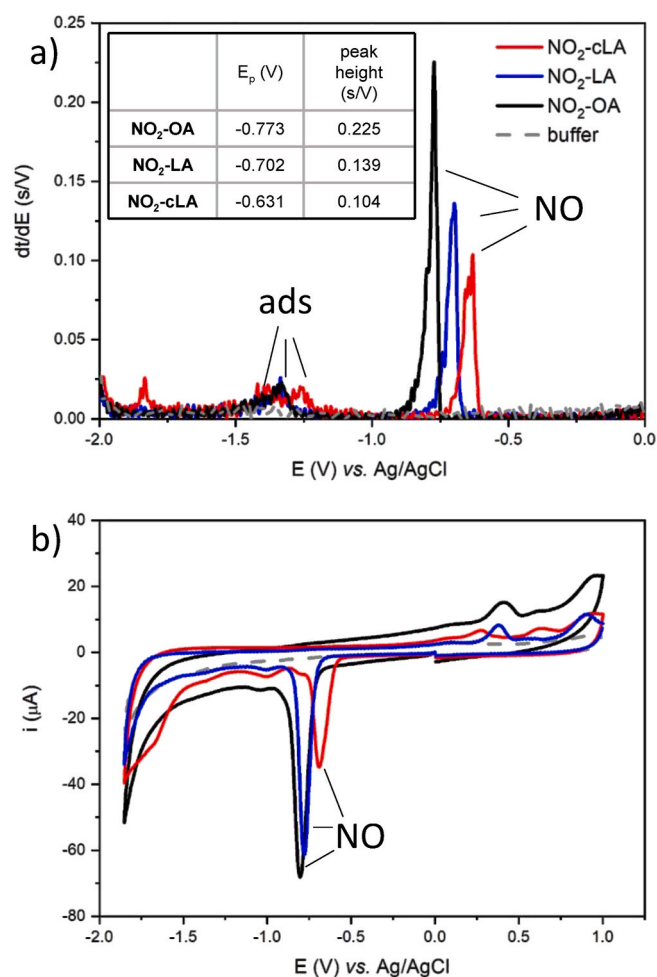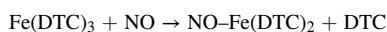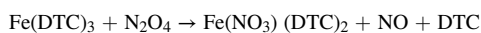

Fig. 2. Chronopotentiometric stripping analysis (CPSA) and alternating current (AC) voltammetry of NO_2-cLA at hanging mercury drop electrode. All measurements were in 0.1 M phosphate buffer at pH 7.4. (a) CPS record of 10 μM NO_2-cLA (blue line) and cLA (red line); i_{str} = −35 μA, time of accumulation t_A = 30 s (E_A = 0 V). (b) In-phase and (c) out-of-phase AC voltammograms of 30 μM NO_2-cLA and cLA; initial (0 V) and end (−1.95 V) potentials, frequency: 66.2 Hz, amplitude: 5 mV, phase angle: 0° (in-phase) and 90° (out-of-phase). For AC voltammetry the electrolyte was degassed for 10 min with argon. (For interpretation of the references to colour in this figure legend, the reader is referred to the Web version of this article.)
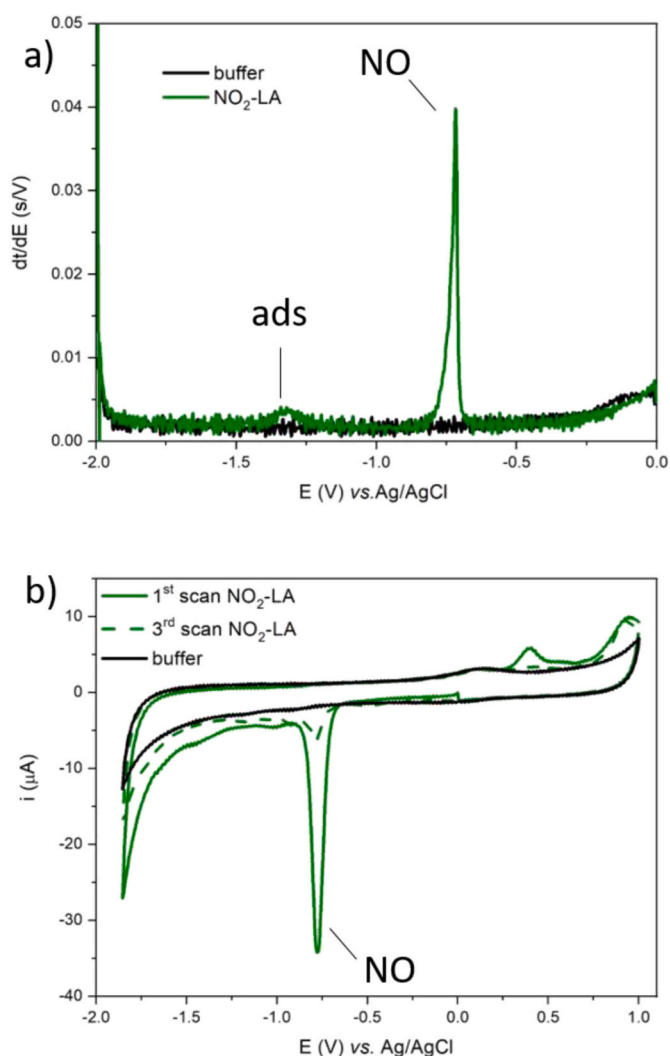
Fig. 3. Chronopotentiometric stripping analysis (CPSA) and cyclic voltammetry (CV) of NO_2-LA. All analyses were performed in 0.1 M phosphate buffer at pH 7.4. (a) CPSA record of 10 μM NO_2-LA at hanging mercury drop electrode; (i_{str} −35 μA). (b) CV of 20 μM NO_2-LA at pyrolytic graphite electrode. CV parameters: initial potential 0 V, first vertex potential −1.85 V, second vertex potential +1 V, step potential 5 mV, scan rate 1 V/s. Time of accumulation t_A = 30 s (E_A = 0 V) was used for both panel a and b. (For interpretation of the references to colour in this figure legend, the reader is referred to the Web version of this article.)

EPR-active complex, resulting in a loss of the EPR signal.

One of the causes for the EPR signal decay of the NO–Fe(II) (DTCS)$_2$ complex may be the reaction between this complex and another ·NO molecule, yielding EPR-silent dinitrosyl species, thus affecting the ·NO trapping efficiency [48]. Also, in spite of all the solutions used for spin trapping procedure were N_2-equilibrated, it is possible that a small fraction of iron from Fe(II) (DTCS)$_2$ was quickly oxidized, giving the Fe (III) (DTCS)$_3$, which is also able to complex with ·NO. Notably, NO–Fe (III) (DTCS)$_3$ can also be converted to NO–Fe(II) (DTCS)$_2$ [49,50]. Accordingly, the extent of Fe^{2+} oxidation to Fe^{3+} and the rate of subsequent steps resulting in the formation of NO–Fe(II) (DTCS)$_2$ complex could also determine the reduction rate of the EPR signal. Finally, dithiocarbamate (DTC)-Fe complexes can also be employed for indirect detection of NO_2/N_2O_4 [51] *via* the following reactions:

$$Fe(DTC)_3 + N_2O_4 \rightarrow Fe(NO_3) (DTC)_2 + NO + DTC$$

$$Fe(DTC)_3 + NO \rightarrow NO\text{–}Fe(DTC)_2 + DTC$$

Fig. 4. Chronopotentiometric stripping analysis (CPSA) and cyclic voltammetry (CV) of NO_2-cLA (red line), NO_2-LA (blue line) and NO_2-OA (black line). All experiments were performed in 0.1 M phosphate buffer at pH 7.4. (a) CPS records of 10 μM NO_2-FA at HMDE; i_{str} −35 μA. Inset table: NO reduction peak potentials and heights. (b) CVs of 20 μM NO_2-FA at PGE. CV parameters: initial potential 0 V, first vertex potential −1.85 V, second vertex potential +1 V, step potential 5 mV, scan rate 1 V/s. Time of accumulation t_A = 30 s (E_A = 0 V) was used for both panel a and b. (For interpretation of the references to colour in this figure legend, the reader is referred to the Web version of this article.)

Thus, the NO–Fe(II) (DTCS)$_2$ complex may arise from both ·NO and ·NO_2 generation by NO_2-FA, especially under aerobic conditions.

3.4. Conformation of NO_2-FA

The MM and QM calculations performed on fatty acids showed that the conformation of aliphatic chain [52–56] is different for saturated versus unsaturated compounds. In saturated chains the *anti* orientation of the C–C–C–C torsion angles (180°) represents the global minimum, whereas its *gauche* orientation (60°) is a local minimum, being less stable than the global one by approx. 2 kJ/mol. The *skew* orientation (120°) belongs to the transition state with a barrier height around 14 kJ/mol.

When a double bond is present in the system, the global minimum is represented by a *skew, skew* conformation of two C–C–C=C dihedrals (*i. e.* like in 3-hexene), also being the case for dienes. In 2,5-heptadiene, a common model for the flexibility of aliphatic chains of FA [53,55], the +*skew*, +*skew* (or -*skew*, -*skew*) orientation is a global minimum. A positive value of the torsion angle corresponds to counterclockwise rotation of the furthest substituent with respect to the central bond. In this conformation, double-bond directions are aligned in parallel, which leads to the extended aliphatic chain. Almost the same stability occurs
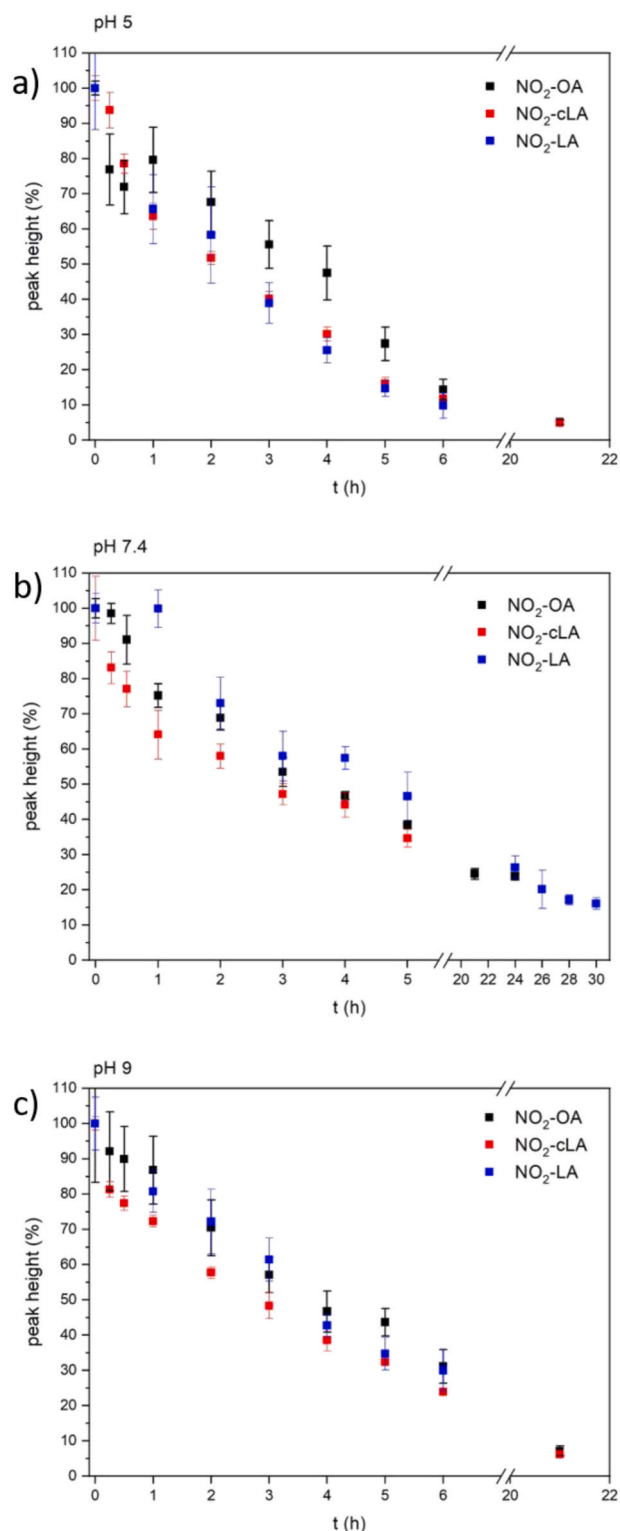
Fig. 5. Time-dependent stability of NO$_2$-FA. Data is represented by the decrease of NO peak height of 8 μM NO$_2$-LA, NO$_2$-cLA and NO$_2$-OA in Britton-Robinson buffer at pH (a) 5, (b) 7.4 and (c) 9 at HMDE. CPSA at i_{str} −35 μA was used in all experiments after a pre-concentration step, time of accumulation t_A = 30 s (E_A = 0 V). (For interpretation of the references to colour in this figure legend, the reader is referred to the Web version of this article.)

for the +*skew, -skew* (or *-skew, +skew*) orientation with the double-bond directions situated perpendicularly, providing more compact (clasped) structure [52].

A nitro substituent does not significantly affect the geometry of aliphatic FA. The most stable conformers of NO$_2$-FA resemble those of non-nitrated FA [56]. For NO$_2$-OA and NO$_2$-LA derivatives, the conformations with +*skew, -skew* combination of C–C–C═C dihedrals are slightly preferred over those with +*skew, +skew* combinations. This could be due to the favorable dispersion interaction between two parts of the aliphatic chains in clasped structures, in comparison with the extended one, which compensates for the energetic superiority of +*skew, +skew* conformation in small model systems. The most visible differences in the structure of NO$_2$-OA compared to OA are smaller absolute values of C–C–C(NO$_2$)═C and C–C–C═C(NO$_2$) dihedral angles in comparison with C–C–C═C torsion angle in FA: the first being 90° and the second 111°. An optimal value 116° was found for native FA [55]. The bulky nitro group probably also increases the barrier height between energy minima for both of the aforementioned conformers.

For NO$_2$-cLA the conformation in the vicinity of double bounds is different, since one *cis*- and one *trans*-C═C bond are in conjugation. This leads at first to slight non-planarity of these two bonds (deviation 5–10°) with an orientation of C–C–C–C (any bond order, starting from the carboxylate, with dihedrals around double bond depicted in **bold**).

For 9-NO$_2$-cLA:

-skew	**cis**	-gauche	**trans**	-skew	(more stable)
+skew	**cis**	-gauche	**trans**	cis	

For 12-NO$_2$-cLA the conformational variability was found even bigger:

-skew	**trans**	-gauche	**cis**	-gauche
cis	**trans**	-gauche	**cis**	+skew
cis	**trans**	+gauche	**cis**	-skew
+skew	**trans**	-gauche	**cis**	-skew

The two most stable energy conformers of NO$_2$-FA and their physical-chemical properties (relative stability, electrostatic potential, HOMO and LUMO) are depicted in Figs. 8–10 and Table 3. From this, it is evident that for all NO$_2$-FA the shape of HOMO and LUMO orbitals is similar, the HOMO orbital is spread around the carboxylic group, whereas the LUMO is composed from contributions in the π* orbitals of the nitro group and of C═C bond(s). The energies of HOMO and LUMO in any given FA are insensitive to the position of the nitro group and its molecular geometry. The increase of polarity of the solvent enlarges the HOMO–LUMO energy gap (by *ca.* 0.35 eV comparing the *n*-octanol and water solvents). The lowest HOMO-LUMO energy gap resulting to the highest reactivity (by 0.2 eV in comparison with other NO$_2$-FA) was found for NO$_2$-cLA what can be caused by the presence of two conjugated C═C bonds in this compound.

3.5. Biological relevance of reported data

Herein three nitro-FA with biological signaling capabilities were biophysically characterized under aqueous conditions. The C-10 isomer of NO$_2$-OA (CXA-10) is being evaluated in Phase 2 clinical trials as a potential new drug candidate [11]. In addition, we have evaluated NO$_2$-LA and its conjugated diene conformer, the latter of significant biological relevance because of its endogenous levels [57]. Comparative redox and EPR analysis indicate NO radical release is a spontaneous decay mechanism for NO$_2$-FA, yet likely does not activate soluble guanylate cyclase to exert physiological responses because of low yields and a kinetically-preferential reaction with nucleophilic amino acid residues [58]. In particular, NO$_2$-FA form adducts with Cys residues of signaling proteins, redox sensors, proteins involved in stress responses and redox-sensitive transcription factors. The important driving factor for
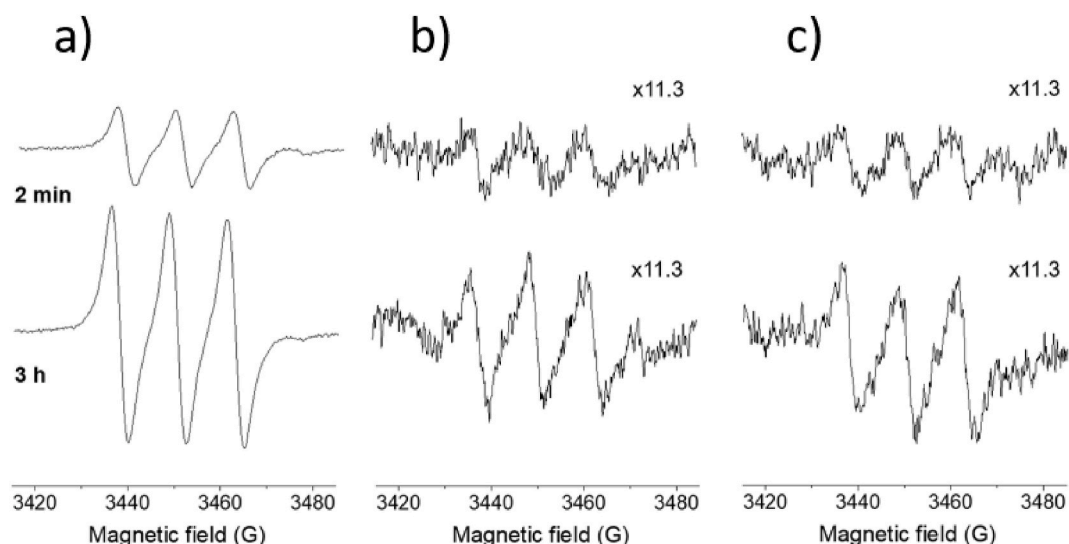
Fig. 6. EPR spectra of NO–Fe(DTCS)$_2$ adducts produced by NO$_2$-FA. Data was obtained after incubation for 2 min and 3 h. (a) NO$_2$-cLA, (b) NO$_2$-LA and (c) NO$_2$-OA.
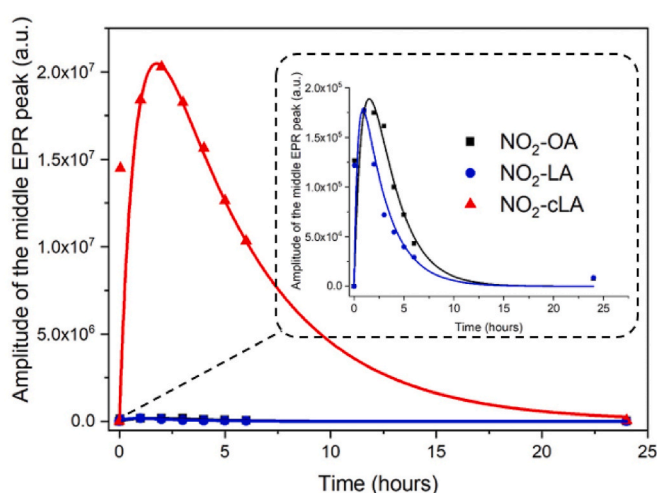

Fig. 7. Kinetics of NO–Fe(DTCS)$_2$ EPR signal intensities. Data was obtained over 24 h. For kinetic measurements, the intensity of the middle EPR peak from the signal triplet was measured. For more details, see the main text.

Table 2
Rate constants for NO release from three different fatty acid nitroalkenes maintained under aqueous conditions.

NO donor	k_1 (arbitrary EPR units/h)
NO$_2$-cLA	$1.3 \cdot 10^6$
NO$_2$-LA	$5.5 \cdot 10^5$
NO$_2$-OA	$5 \cdot 10^5$

these low molecular weight nucleophile (*i.e.*, GSH) or protein alkylation reactions will be steric hindrance, specifically the availability and reactivity of particular Cys residues with NO$_2$-FA.

The structural data from this study can facilitate the study and prediction of downstream NO$_2$-FA reactions. For example, the *p*Ka of Cys targets is crucial factor [58], since thiolate anions are so readily nitroalkylated. The involvement of vicinal basic residues that promote Cys deprotonation is also critical and under investigation. Another key parameter that defines downstream signaling responses will be the stability of NO$_2$-FA in plasma and at cellular and tissue levels. At the same time, excessive protein target accumulation of NO$_2$-FA can become

Fig. 8a. Physico-chemical properties of 9-NO$_2$-OA presented for two most stable conformers (I, II). From top to bottom: molecular electrostatic potential (ESP); the highest occupied molecular orbital (HOMO); the lowest unoccupied molecular orbital (LUMO).
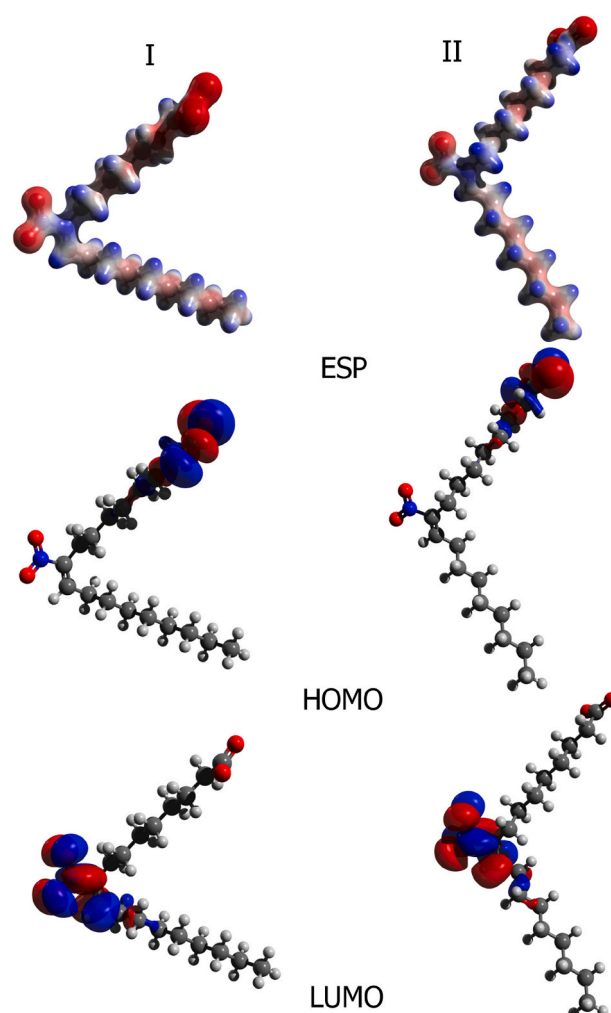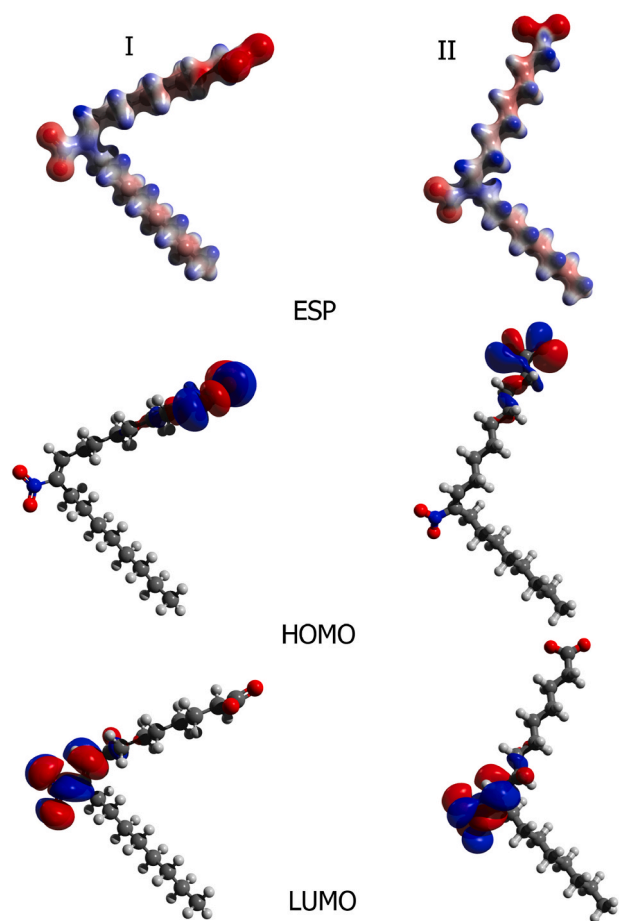
Fig. 8b. Physico-chemical properties of 10-NO$_2$-OA presented for two most stable conformers (I, II). From top to bottom: molecular electrostatic potential (ESP); the highest occupied molecular orbital (HOMO); the lowest unoccupied molecular orbital (LUMO).

relationship between the degradation of NO$_2$-FA and the aqueous ·NO release phenomenon is documented by the comparison of 24 h CPSA-degradation profiles in Fig. 5, which fits the EPR-degradation kinetics shown in Fig. 7. It is viewed that the generation of NO by all nitroalkenes will be a consequence of aqueous decay *via* a modified Nef reaction, a phenomenon reported for in nitroalkene derivatives of bis-allylic linoleic acid [20]. Herein, we suggest that conjugated diene-containing FA nitroalkenes are also capable of undergoing the same protonation-deprotonation cycle followed by reaction with the hydroxide anion always present in aqueous milieu. Because of the adjacent conjugated double bonds in NO$_2$-cLA, it is viewed that the nitroso intermediate would have a weaker C–N bond and thus be more susceptible to scission to yield NO radical. Prior mass spectrometric

Fig. 9. Physico-chemical properties of 10-NO$_2$-LA presented for two most stable conformers (I, II). From top to bottom: molecular electrostatic potential (ESP); the highest occupied molecular orbital (HOMO); the lowest unoccupied molecular orbital (LUMO).
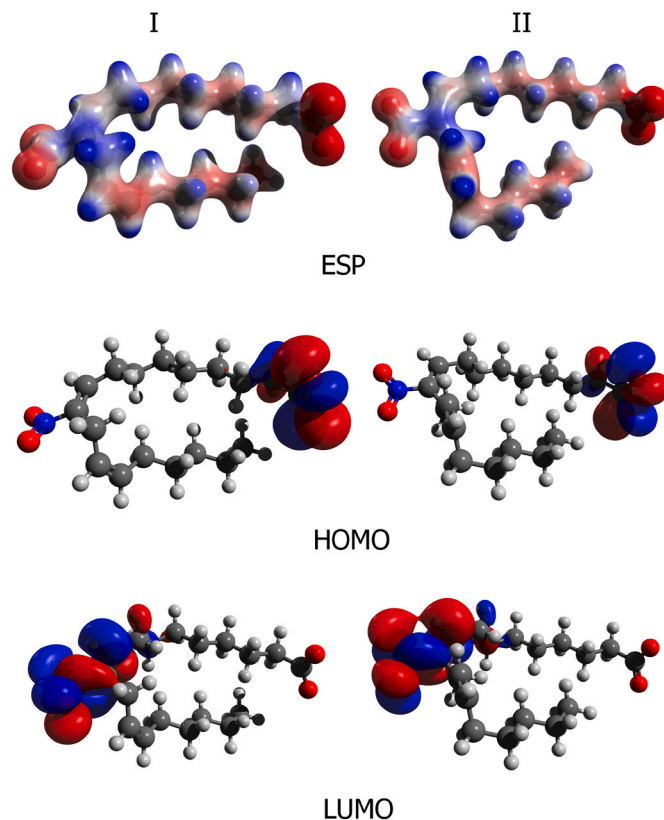
toxic, compromising their action as signaling molecules. In this regard, enzymatic reduction of the nitroalkene, mitochondrial β-oxidation, NO$_2$-FA incorporation into complex lipids such as triglycerides and the concerted GSH alkylation and export by multi-drug resistant proteins can limit toxic accumulation of this class of lipid electrophiles [59–63].

Depending on buffer, media or *in vivo* conditions, NO$_2$-FA are stable for several minutes to several hours [11,64]. This time perspective corresponds very well to the pharmacokinetics that would support activation of the expression of adaptive signaling-related genes and the modulation of both acute and chronic inflammatory responses [65]. The

Table 3

Relative energies and HOMO-LUMO characteristics of two most stable conformers of studied NO$_2$–FAs in different solvents. All calculations were performed at B3LYP/6–311++G (d, p) level of theory. For geometry of conformers see Figs. 8–10.

	Water				Methanol				*n*-Octanol			
	ΔE[a]	EHOMO[b]	ELUMO[c]	LUMO-HOMO[d]	ΔE[a]	EHOMO[b]	ELUMO[c]	LUMO-HOMO[d]	ΔE[a]	EHOMO[b]	ELUMO[c]	LUMO-HOMO[d]
12-NO$_2$-cLA	0.00	−8.287	−0.953	7.334	0.00	−8.191	−0.956	7.235	0.00	−7.813	−0.851	6.962
	2.15	−8.289	−0.981	7.308	2.06	−8.192	−0.954	7.238	1.84	−7.816	−0.851	6.965
9-NO$_2$-cLA	0.00	−8.288	−0.893	7.395	0.23	−8.187	−0.863	7.324	0.58	−7.807	−0.749	7.058
	0.01	−8.302	−0.970	7.332	0.00	−8.197	−0.947	7.250	0.00	−7.811	−0.828	6.983
10-NO$_2$-LA	0.00	−8.297	−0.737	7.560	0.00	−8.197	−0.708	7.489	0.00	−7.817	−0.590	7.227
	7.48	−8.297	−0.804	7.493	7.54	−8.197	−0.776	7.421	8.02	−7.814	−0.665	7.149
9-NO$_2$-OA	0.00	−8.286	−0.774	7.512	0.00	−8.188	−0.745	7.443	0.00	−7.808	−0.621	7.187
	0.02	−8.285	−0.774	7.511	0.02	−8.187	−0.746	7.441	1.08	−7.807	−0.636	7.171
10-NO$_2$-OA	0.00	−8.287	−0.758	7.529	0.00	−8.190	−0.731	7.459	0.00	−7.816	−0.627	7.189
	1.02	−8.286	−0.771	7.515	1.00	−8.190	−0.744	7.446	0.96	−7.815	−0.640	7.175

[a] relative energy of the conformers (in kJ/mol).
[b,c,d] HOMO, LUMO energy and their difference (all in eV).

Fig. 10a. Physico-chemical properties of 9-NO$_2$-cLA presented for two most stable conformers (I, II). From top to bottom: molecular electrostatic potential (ESP); the highest occupied molecular orbital (HOMO); the lowest unoccupied molecular orbital (LUMO).
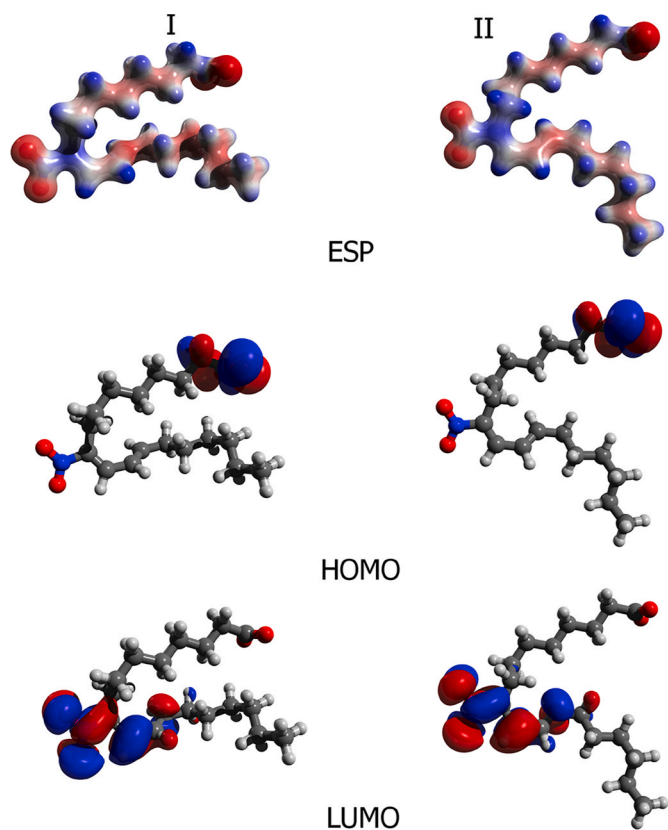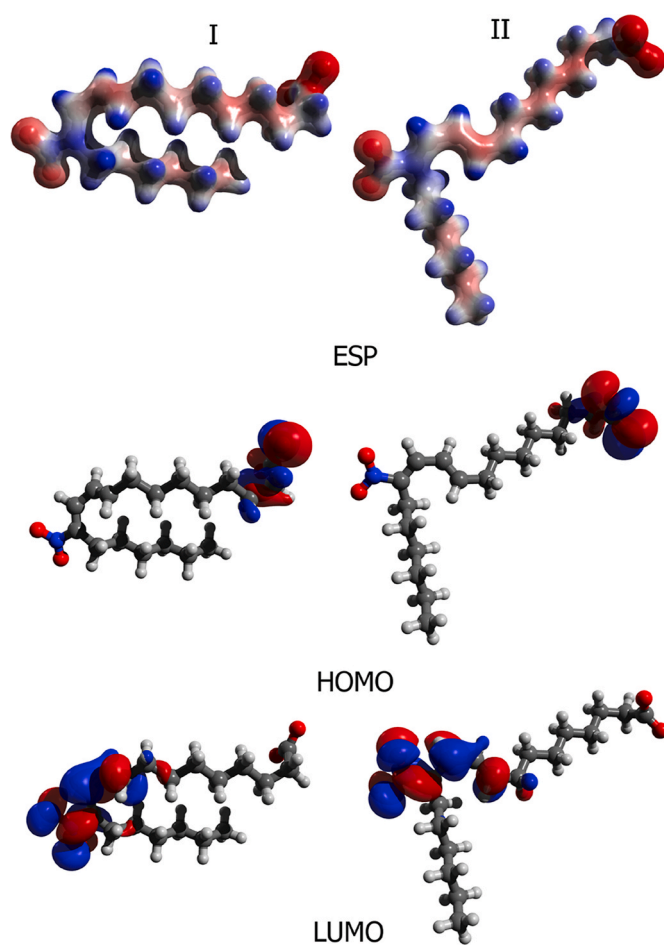

Fig. 10b. Physico-chemical properties of 12-NO$_2$-cLA presented for two most stable conformers (I, II). From top to bottom: molecular electrostatic potential (ESP); the highest occupied molecular orbital (HOMO); the lowest unoccupied molecular orbital (LUMO).

detection of the expected oxidized fatty acid products and the present direct detection of NO formation support this pathway of nitroalkene decay. This acid/base chemistry may potentially be employed by enzymes that might also catalyze NO release from the multiple lipid nitroalkene derivatives that have been detected biologically. It is noted in the latter context however that the main physiological reaction pathway for NO$_2$-cLA is more likely to be a) stabilization by esterification into complex lipids, b) incorporation into hydrophobic compartments such as hydrophobic pockets of proteins, micelles, chylomicrons, lipid droplets or membranes that will in turn limit protonation-deprotonation of the nitroalkene and subsequent NO formation and c) the alkylation of proteins that in turn also inhibits the chemistries associated with the Nef reaction.

NO$_2$-FA are generated by the reactions of unsaturated FA with ·NO, and NO$_2$-derived nitrating species (Scheme 2). The life-time of these species are all very short, *e.g.* for ONOO-, a $t_{1/2}$ of 0.15 s was reported [66]. The generation of these species can be upregulated by inflammation, metabolism and other physiological and pathological manifestations [67]. One common denominator is that these reactive species act vicinal to the location where they are generated, with further distribution limited by a low $t_{1/2}$ and high reactivity. In contrast, the nitration of unsaturated FA to a more stable product results in broader distribution and more systemic signaling potential. Thus, the transformation of various nitrogen oxides to ·NO$_2$ and the formation of NO$_2$-FA transduces the effects of often toxic mediators of inflammation into a species that induces adaptive metabolic and gene expression responses. The relationship between the stability and biological reactivity of NO$_2$-FA in the context of their origin, distribution and storage is depicted in Scheme 2.

4. Conclusions

This study affirms that NO$_2$-FA biological actions are pleiotropic and that understanding the physicochemical properties of NO$_2$-FA is crucial for clearer insight into the mechanisms of action of these electrophilic products of inflammation and metabolism. Despite a number of pharmacological and clinical studies [68], only limited studies describe the structure, stability and reactivity of NO$_2$-FA.

NO$_2$-FA are electrochemically reducible around −0.8 V, which corresponding to reduction of R–NO$_2$ group. Based on the potential of reduction peak NO we can evaluate electrophilic capacity or reactivity of NO$_2$-FA, which decreases, with NO$_2$-cLA >> NO$_2$-LA > NO$_2$-OA. This electrochemical data is in good agreement with DFT calculations. In this respect, the correlation of LUMO energy and the peak NO potential is an important parameter. The LUMO energy of the tested derivatives ranges from −0.7 to −0.95 eV and, the electron deficient region is located at the R–NO$_2$ group for all compounds studied. Furthermore, the mechanism of NO release [69] was investigated by EPR spectroscopy. The formation of ·NO or ·NO$_2$ radicals is due to the spontaneous degradation of NO$_2$-FA. A highly efficient donor of NO radical(s) is NO$_2$-cLA, for which a rate constant for radical(s) formation of $1.3 \cdot 10^6$ was observed. This value differs from the rate constants for NO$_2$-LA and NO$_2$-OA by one order of magnitude. From theoretical studies [70] as well as from pharmacological studies of adipose tissue [71], it is evident that NO$_2$-FA exhibit different behavior when they are an integral part of organized lipid structures such as membranes, micelles, chylomicrons and lipid droplets
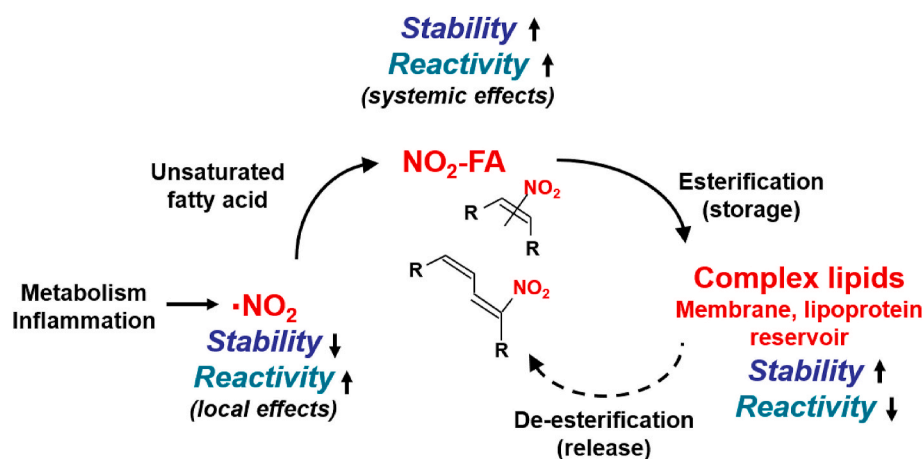
Scheme 2. Relationships between the stability and reactivity of NO$_2$-FA in the context of their origin and distribution. Nitrogen dioxide radical, generated by diverse metabolic and inflammatory reactions (ref. [68]) reacts with bis-allylic or conjugated diene-containing unsaturated fatty acids to yield electrophilic NO$_2$-FA. These nitroalkenes and many of their metabolites are more stable than the reactive oxygen or nitrogen oxide species that serve as their precursors. Finally, the reversible esterification of NO$_2$-FA into complex lipids and micellar, lipoprotein, lipid droplet or membrane structures stabilizes these species.

or if they are freely available in solution (Scheme 2). This has to be taken into account with respect to the stability of the NO$_2$-FA in various model systems.

When working in an aqueous environment, the concentration of NO$_2$-FA also plays an important role, because of self-assembly processes [43]. If the concentration of NO$_2$-FA is lower than the CMC, monomeric fractions are present in the solution. Conversely, when the CMC is exceeded, the NO$_2$-FA monomers are transformed into self-assembled structures, most often liposome-like micelles. In the native (non-pathological) cellular environment, free NO$_2$-FA can be found at nM, or sub-nM, concentrations [64]. Thus, when conducting an *in vitro* experiment with μM NO$_2$-FA concentrations, it is important to take into account micellization, vesicle formation, and aggregation phenomena.

Defining the endogenous or pharmacological actions of the heterogeneous and pleiotropically-acting NO$_2$-FA class requires a comprehensive and multi-disciplinary approach. In particular, conformational polymorphism is an inseparable property of NO$_2$-FA where, in addition to the positional isomers, we have to consider *cis/trans* isomerism and the formation of "open" and "closed" conformer populations [54]. These will achieve a dynamically changing equilibrium in the aqueous solution depending on the experimental conditions. In general, the presence of the nitro group has a rather negligible effect on the conformation of NO$_2$-FA as compared to unsubstituted FA, but a profound effect on chemical reactivity and downstream effects.

Declaration of interests

The authors declare that they have no known competing financial interests or personal relationships that could have appeared to influence the work reported in this paper.

Declaration of competing interest

B.A.F. acknowledges financial interest in Complexa, Inc. and Creegh Pharmaceuticals.

Acknowledgments

References

[1] S. Kalyanaraman, Nitrated lipids: a class of cell-signaling molecules, Proc. Natl. Acad. Sci. U.S.A. 101 (2004) 11527–11528.

[2] M. Delmastro-Greenwood, B.A. Freeman, S.G. Wendell, Redox-dependent anti-inflammatory signaling actions of unsaturated fatty acids, Annu. Rev. Physiol. 76 (2014) 79–105.

[3] S. Bartesaghi, R. Radi, Fundamentals on the biochemistry of peroxynitrite and protein tyrosine nitration, Redox Biol 14 (2018) 618–625.

[4] C. Bregere, I. Rebrin, R.S. Sohal, Detection and characterization of *in vivo* nitration and oxidation of tryptophan residues in proteins, Methods Enzymol. 441 (2008) 339–349.

[5] J. Khan, D.M. Brennan, N. Bradley, B. Gao, R. Bruckdorfer, M. Jacobs, 3-Nitrotyrosine in the proteins of human plasma determined by an ELISA method, Biochem. J. 330 (1998) 795–801.

[6] D. Tsikas, A.A. Zoerner, J. Jordan, Oxidized and nitrated oleic acid in biological systems: analysis by GC-MS/MS and LC-MS/MS, and biological significance, Biochim. Biophys. Acta 1811 (2011) 694–705.

[7] P.R.S. Baker, F.J. Schopfer, S. Sweeney, B.A. Freeman, Red cell membrane and plasma linoleic acid nitration products: synthesis, clinical identification, and quantitation, Proc. Natl. Acad. Sci. U.S.A. 101 (2004) 11577–11582.

[8] M. Balazy, C.D. Poff, Biological nitration of arachidonic acid, Curr. Vasc. Pharmacol. 2 (2004) 81–93.

[9] A.J. Deen, V. Sihvola, J. Harkonen, T. Patinen, S. Adinolfi, A.L. Levonen, Regulation of stress signaling pathways by nitro-fatty acids, Nitric Oxide : biology and chemistry 78 (2018) 170–175.

[10] T. Melo, J.F. Montero-Bullon, P. Domingues, M.R. Domingues, Discovery of bioactive nitrated lipids and nitro-lipid-protein adducts using mass spectrometry-based approaches, Redox Biol 23 (2019) 101106.

[11] F.J. Schopfer, D.A. Vitturi, D.K. Jorkasky, B.A. Freeman, Nitro-fatty acids: new drug candidates for chronic inflammatory and fibrotic diseases, Nitric Oxide : biology and chemistry 79 (2018) 31–37.

[12] B.A. Freeman, M. Pekarova, H. Rubbo, A. Trostchansky, Electrophilic nitro-fatty acids: nitric oxide and nitrite-derived metabolic and inflammatory signaling mediators, in: L.J. Ignarro, B.A. Freeman (Eds.), Nitric Oxide: Biology and Pathobiology, third ed., Elsevier, London, England, 2017, pp. 213–229.

[13] F.A. Carey, R.J. Sundberg, Advanced Organic Chemistry: Part B: Reaction and Synthesis, fifth ed., Springer US, 2007.

[14] L. Turell, D.A. Vitturi, E.L. Coitino, L. Lebrato, M.N. Moller, C. Sagasti, S. R. Salvatore, S.R. Woodcock, B. Alvarez, F.J. Schopfer, The chemical basis of thiol addition to nitro-conjugated linoleic acid, a protective cell-signaling lipid, J. Biol. Chem. 292 (2017) 1145–1159.

[15] P.R.S. Baker, F.J. Schopfer, V.B. O'Donnell, B.A. Freeman, Convergence of nitric oxide and lipid signaling: anti-inflammatory nitro-fatty acids, Free Radic. Biol. Med. 46 (2009) 989–1003.

[16] F.J. Schopfer, C. Cipollina, B.A. Freeman, Formation and signaling actions of electrophilic lipids, Chem. Rev. 111 (2012) 5997–6021.

[17] C. Batthyany, F.J. Schopfer, P.R.S. Baker, R. Duran, L.M.S. Baker, Y. Huang, C. Cervenansky, B.P. Branchaud, B.A. Freeman, Reversible post-translational modification of proteins by nitrated fatty acids in vivo, J. Biol. Chem. 281 (2006) 20450–20463.

[18] M.J. Gorczynski, J. Huang, H. Lee, S.B. King, Evaluation of nitroalkenes as nitric oxide donors, Bioorg. Med. Chem. Lett 17 (2007) 2013–2017.

[19] D.G. Lim, S. Sweeney, A. Bloodsworth, C.R. White, P.H. Chumley, N.R. Krishna, F. Schopfer, V.B. O'Donnell, J.P. Eiserich, B.A. Freeman, Nitrolinoleate, a nitric oxide-derived mediator of cell function: synthesis, characterization, and vasomotor activity, Proc. Natl. Acad. Sci. U.S.A. 99 (2002) 15941–15946.

[20] F.J. Schopfer, P.R.S. Baker, G. Giles, P. Chumley, C. Batthyany, J. Crawford, R. P. Patel, N. Hogg, B.P. Branchaud, J.R. Lancaster Jr., B.A. Freeman, Fatty acid transduction of nitric oxide signaling: nitrolinoleic acid is a hydrophobically stabilized nitric oxide donor, J. Biol. Chem. 280 (2005) 19289–19297.

[21] E.S. Lima, M.G. Bonini, O. Augusto, H.V. Barbeiro, H.P. Souza, D.S.P. Abdalla, Nitrated lipids decompose to nitric oxide and lipid radicals and cause vasorelaxation, Free Radic. Biol. Med. 39 (2005) 532–539.

[22] R. Cammack, C.L. Joannou, X.Y. Cui, C. Torres Martinez, S.R. Maraj, M.N. Hughes, Nitrite and nitrosyl compounds in food preservation, Biochim. Biophys. Acta 1411 (1999) 475–488.

[23] K.S. Hughan, S.G. Wendell, M. Delmastro-Greenwood, N. Helbling, C. Corey, L. Bellavia, G. Potti, G. Grimes, B. Goodpaster, D.B. Kim-Shapiro, S. Shiva, B. A. Freeman, M.T. Gladwin, Conjugated linoleic acid modulates clinical responses to oral nitrite and nitrate, Hypertension 70 (2017) 634–644.

[24] M. Fazzari, A. Trostchansky, F.J. Schopfer, S.R. Salvatore, B. Sanchez-Calvo, D. Vitturi, R. Valderrama, J.B. Barroso, R. Radi, B.A. Freeman, H. Rubbo, Olives and olive oil are sources of electrophilic fatty acid nitroalkenes, PloS One 9 (2014), e84884.

[25] R.L. Charles, O. Rudyk, O. Prysyazhna, A. Kamynina, J. Yang, C. Morisseau, B. D. Hammock, B.A. Freeman, P. Eaton, Protection from hypertension in mice by the Mediterranean diet is mediated by nitro fatty acid inhibition of soluble epoxide hydrolase, Proc. Natl. Acad. Sci. U.S.A. 111 (2014) 8167–8172.

[26] S.M. Nadtochiy, E.K. Redman, Mediterranean diet and cardioprotection: the role of nitrite, polyunsaturated fatty acids, and polyphenols, Nutrition 27 (2011) 733–744.

[27] G.J. Buchan, G. Bonacci, M. Fazzari, S.R. Salvatore, S. Gelhaus Wendell, Nitro-fatty acid formation and metabolism, Nitric Oxide : biology and chemistry 79 (2018) 38–44.

[28] M. Balazy, T. Iesaki, J.L. Park, H. Jiang, P.M. Kaminski, M.S. Wolin, Vicinal nitrohydroxyeicosatrienoic acids: vasodilator lipids formed by reaction of nitrogen dioxide with arachidonic acid, J. Pharmacol. Exp. Therapeut. 299 (2001) 611–619.

[29] D. Tsikas, A.A. Zoerner, A. Mitschke, F.M. Gutzki, Nitro-fatty acids occur in human plasma in the picomolar range: a targeted nitro-lipidomics GC-MS/MS study, Lipids 44 (2009) 855–865.

[30] L.M.S. Baker, P.R.S. Baker, F. Golin-Bisello, F.J. Schopfer, M. Fink, S.R. Woodcock, B.P. Branchaud, R. Radi, B.A. Freeman, Nitro-fatty acid reaction with glutathione and cysteine: kinetic analysis of thiol alkylation by a Michael addition reaction, J. Biol. Chem. 282 (2007) 31085–31093.

[31] M. Zatloukalova, M. Mojovic, A. Pavicevic, M. Kabelac, B.A. Freeman, M. Pekarova, J. Vacek, Redox properties and human serum albumin binding of nitro-oleic acid, Redox Biol 24 (2019) 101213.

[32] S.R. Woodcock, G. Bonacci, S.L. Gelhaus, F.J. Schopfer, Nitrated fatty acids: synthesis and measurement, Free Radic. Biol. Med. 59 (2013) 14–26.

[33] T.F. Zhu, I. Budin, J.W. Szostak, Preparation of fatty acid micelles, Methods Enzymol. (2013) 283–288.

[34] A. Chattopadhyay, E. London, Fluorimetric determination of critical micelle concentration avoiding interference from detergent charge, Anal. Biochem. 139 (1984) 408–412.

[35] C. Mongay, V. Cerda, A Britton-Robinson buffer of known ionic strength, Ann. Chim. 64 (1974) 409–412.

[36] M.A. Miteva, F. Guyon, P. Tuffery, Frog2: efficient 3D conformation ensemble generator for small compounds, Nucleic Acids Res. 38 (2010) W622–W627.

[37] M.D. Hanwell, D.E. Curtis, D.C. Lonie, T. Vandermeerschd, E. Zurek, G. R. Hutchison, Avogadro: an advanced semantic chemical editor, visualization, and analysis platform, J. Cheminf. 4 (2012) 17.

[38] G. Scalmani, M.J. Frisch, Continuous surface charge polarizable continuum models of solvation. I. General formalism, J. Chem. Phys. 132 (2010) 114110.

[39] M.J. Frisch, G.W. Trucks, H.B. Schlegel, G.E. Scuseria, M.A. Robb, J.R. Cheeseman, G. Scalmani, V. Barone, G.A. Petersson, H. Nakatsuji, X. Li, M. Caricato, A.V. Marenich, J. Bloino, B.G. Janesko, R. Gomperts, B. Mennucci, H.P. Hratchian, J.V. Ortiz, A.F. Izmaylov, J.L. Sonnenberg, Williams, F. Ding, F. Lipparini, F. Egidi, J. Goings, B. Peng, A. Petrone, T. Henderson, D. Ranasinghe, V.G. Zakrzewski, J. Gao, N. Rega, G. Zheng, W. Liang, M. Hada, M. Ehara, K. Toyota, R. Fukuda, J. Hasegawa, M. Ishida, T. Nakajima, Y. Honda, O. Kitao, H. Nakai, T. Vreven, K. Throssell, J.A. Montgomery Jr, J.E. Peralta, F. Ogliaro, M.J. Bearpark, J.J. Heyd, E. N. Brothers, K.N. Kudin, V.N. Staroverov, T.A. Keith, R. Kobayashi, J. Normand, K. Raghavachari, A.P. Rendell, J.C. Burant, S.S. Iyengar, J. Tomasi, M. Cossi, J.M. Millam, M. Klene, C. Adamo, R. Cammi, J.W. Ochterski, R.L. Martin, K. Morokuma, O. Farkas, J.B. Foresman, D.J. Fox, Gaussian 16 Rev. C.01, (Wallingford, CT).

[40] A.L. Fameau, A. Arnould, A. Saint-Jalmes, Responsive self-assemblies based on fatty acids, Curr. Opin. Colloid Interface Sci. 19 (2014) 471–479.

[41] G.V. Richieri, R.T. Ogata, A.M. Kleinfeld, A fluorescently labeled intestinal fatty acid binding protein. Interactions with fatty acids and its use in monitoring free fatty acids, J. Biol. Chem. 267 (1992) 23495–23501.

[42] M. Delample, F. Jerome, J. Barrault, J.P. Douliez, Self-assembly and emulsions of oleic acid-oleate mixtures in glycerol, Green Chem. 13 (2011) 64–68.

[43] Y. Fan, Y. Fang, L. Ma, H. Jiang, Investigation of micellization and vesiculation of conjugated linoleic acid by means of self-assembling and self-crosslinking, J. Surfactants Deterg. 18 (2015) 179–188.

[44] B.A. Freeman, P.R.S. Baker, F.J. Schopfer, S.R. Woodcock, A. Napolitano, M. D'Ischia, Nitro-fatty acid formation and signaling, J. Biol. Chem. 283 (2008) 15515–15519.

[45] C. Kraiya, P. Singh, Z.V. Todres, D.H. Evans, Voltammetric studies of the reduction of *cis*- and *trans*-alpha-nitrostilbene, J. Electroanal. Chem. 563 (2004) 171–180.

[46] A.J. Bard, L.R. Faulkner, Electrochemical Methods: Fundamentals and Applications, John Willey & Sons, New York, USA, 2001.

[47] L. Havran, S. Billova, E. Palecek, Electroactivity of avidin and streptavidin. Avidin signals at mercury and carbon electrodes respond to biotin binding, Electroanalysis 16 (2004) 1139–1148.

[48] T. Yoshimura, Y. Kotake, Spin trapping of nitric oxide with the iron-dithiocarbamate complex: chemistry and biology, Antioxidants Redox Signal. 6 (2004) 639–647.

[49] S. Fujii, K. Kobayashi, S. Tagawa, T. Yoshimura, Reaction of nitric oxide with the iron(III) complex of *N*-(dithiocarboxy)sarcosine: a new type of reductive nitrosylation involving iron(IV) as an intermediates, J. Chem. Soc. Dalton Trans. (2000) 3310–3315.

[50] T. Nagano, T. Yoshimura, Bioimaging of nitric oxide, Chem. Rev. 102 (2002) 1235–1269.

[51] N.D. Yordanov, V. Iliev, D. Shopov, A. Jezierski, B. Jezoswka-Trzebiatowska, Studies of the intermolecular interactions of metal chelate complexes. II. EPR study on the interactions of metal chelate complexes NOx (x = 1 or 2), Inorg. Chim. Acta. 60 (1982) 9–15.

[52] K.R. Applegate, J.A. Glomset, Computer-based modeling of the conformation and packing properties of docosahexaenoic acid, J. Lipid Res. 27 (1986) 658–680.

[53] S.E. Feller, K. Gawrisch, A.D. MacKerell Jr., Polyunsaturated fatty acids in lipid bilayers: intrinsic and environmental contributions to their unique physical properties, J. Am. Chem. Soc. 124 (2002) 318–326.

[54] T. Gocen, S. Haman Bayari, M. Haluk Guven, Linoleic acid and its potassium and sodium salts: a combined experimental and theoretical study, J. Mol. Struct. 1150 (2017) 68–81.

[55] J.B. Klauda, V. Monje, T. Kim, W. Im, Improving the CHARMM force field for polyunsaturated fatty acid chains, J. Phys. Chem. B 116 (2012) 9424–9431.

[56] M.R. Rich, Conformational analysis of arachidonic and related fatty acids using molecular dynamics simulations, Biochim. Biophys. Acta BBA - Mol. Cell Res. 1178 (1993) 87–96.

[57] F.J. Schopfer, N.K.H. Khoo, Nitro-fatty acid logistics: formation, biodistribution, signaling, and pharmacology, Trends Endocrinol. Metabol. 30 (2019) 505–519.

[58] L. Turell, M. Steglich, B. Alvarez, The chemical foundations of nitroalkene fatty acid signaling through addition reactions with thiols, Nitric Oxide : biology and chemistry 78 (2018) 161–169.

[59] R.L. Alexander, D.J.P. Bates, M.W. Wright, S.B. King, C.S. Morrow, Modulation of nitrated lipid signaling by multidrug resistance protein 1 (MRP1): glutathione conjugation and MRP1-mediated efflux inhibit nitrolinoleic acid-induced, PPARϒ-dependent transcription activation, Biochemistry 45 (2006) 7889–7896.

[60] M. Fazzari, N. Khoo, S.R. Woodcock, L. Li, B.A. Freeman, F.J. Schopfer, Generation and esterification of electrophilic fatty acid nitroalkenes in triacylglycerides, Free Radic. Biol. Med. 87 (2015) 113–124.

[61] S.R. Salvatore, D.A. Vitturi, P.R.S. Baker, G. Bonacci, J.R. Koenitzer, S. R. Woodcock, B.A. Freeman, F.J. Schopfer, Characterization and quantification of endogenous fatty acid nitroalkene metabolites in human urine, J. Lipid Res. 54 (2013) 1998–2009.

[62] D.A. Vitturi, C.S. Chen, S.R. Woodcock, S.R. Salvatore, G. Bonacci, J.R. Koenitzer, N.A. Stewart, N. Wakabayashi, T.W. Kensler, B.A. Freeman, F.J. Schopfer, Modulation of nitro-fatty acid signaling prostaglandin reductase-1 is a nitroalkene reductase, J. Biol. Chem. 288 (2013) 25626–25637.

[63] S.R. Woodcock, S.G. Wendell, F.J. Schopfer, B.A. Freeman, Synthesis of an electrophilic keto-tetraene 15-oxo-Lipoxin A4 methyl ester via a MIDA boronate, Tetrahedron Lett. 59 (2018) 3524–3527.

[64] S.R. Salvatore, D.A. Vitturi, M. Fazzari, D.K. Jorkasky, F.J. Schopfer, Evaluation of 10-nitro oleic acid bio-elimination in rats and humans, Sci. Rep. 7 (2017) 39900.

[65] I. Lesur, J. Textoris, B. Loriod, C. Courbon, S. Garcia, M. Leone, C. Nguyen, Gene expression profiles characterize inflammation stages in the acute lung injury in mice, PloS One 5 (2010) 1–14.

[66] C. Schoneich, Kinetics of thiol reactions, Methods Enzymol. (1995) 45–55.

[67] C.C. Winterbourn, Reconciling the chemistry and biology of reactive oxygen species, Nat. Chem. Biol. 4 (2008) 278–286.

[68] B.A. Freeman, V.B. O'Donnell, F.J. Schopfer, The discovery of nitro-fatty acids as products of metabolic and inflammatory reactions and mediators of adaptive cell signaling, Nitric Oxide : biology and chemistry 77 (2018) 106–111.

[69] Y.H. Su, S.S. Wu, C.H. Hu, Release of nitric oxide from nitrated fatty acids: insights from computational chemistry, J. Chin. Chem. Soc. 66 (2019) 41–48.

[70] J. Franz, T. Bereau, S. Pannwitt, V. Anbazhagan, A. Lehr, U. Nubbemeyer, U. Dietz, M. Bonn, T. Weidner, D. Schneider, Nitrated fatty acids modulate the physical properties of model membranes and the structure of transmembrane proteins, Chem. Eur. J. 23 (2017) 9690–9697.

[71] M. Fazzari, N.K.H. Khoo, S.R. Woodcock, D.K. Jorkasky, L. Li, F.J. Schopfer, B. A. Freeman, Nitro-fatty acid pharmacokinetics in the adipose tissue compartment, J. Lipid Res. 58 (2017) 375–385.